LASER DOPPLER INVESTIGATION OF SOURCE LOCATION EFFECTS ON NEAR-ORIFICE FLOW AND ACOUSTIC VELOCITY FIELD OVER A LINER

Ludovic Ambrosiani[1,2], Fabien Mery[1], Estelle Piot[1], Francesco Avallone[2]
[1] *DMPE, ONERA, Université de Toulouse, 31000, Toulouse, France*
[2] *Politecnico di Torino, Corso Duca degli Abruzzi 24, 10129, Torino, Italy*

Abstract

The interaction between acoustic waves and turbulent grazing flow over liners strongly affects their aeroacoustic performance. This study experimentally investigates the influence of acoustic source propagation direction relative to the mean flow on near-orifice flow dynamics and liner response using laser doppler velocimetry (LDV) in ONERA's Aero-Thermo-Acoustic facility, providing high-resolution velocity measurements. The analysis focuses on the region close to an orifice, where coupling between the turbulent boundary layer and the acoustic field is the strongest. Mean and root-mean-square (RMS) velocities are examined together with the acoustic-induced velocity field, extracted from LDV data by cross-correlation with a reference source signal, allowing the determination of both amplitude and phase. The results show that source position affects the near-orifice response even where the two configurations have comparable total SPL. Upstream forcing produces stronger wall-normal coherent motion over the aperture and a larger coupling between the streamwise and wall-normal velocity components. The phase-resolved measurements further suggest changes in the shape and orientation of the periodic trajectory followed by the coherent velocity vector. These findings indicate that source direction influences not only the acoustic level along the liner, but also the local flow–acoustic structure at the orifice scale.

Keywords: *Aeroacoustic, Liner, Turbulent Flow, Laser Doppler Velocimetry*

Corresponding author: *ludovic.ambrosiani@polito.it.*

1. Introduction

Acoustic liners are widely used in aero-engine nacelles to reduce fan and broadband noise emissions, particularly under grazing-flow conditions representative of realistic operating environments [1], [2]. Their acoustic response is commonly described in terms of surface impedance, but this quantity often relies on simplifying assumptions regarding local reaction, spatial homogeneity, and the treatment of the turbulent boundary layer above the liner surface [3], [4], [5], [6]. These assumptions become increasingly restrictive when high sound pressure levels, grazing flow, or small geometrical features of the perforations modify the local flow-acoustic coupling [7], [8], [9].

At the scale of the perforations, liner performance is governed by the interaction between the acoustic-induced motion through the orifices, vortex shedding at the aperture edges, and the turbulent boundary layer developing over the facesheet [10], [11]. Recent numerical studies have shown that the grazing-flow development can alter the boundary-layer displacement thickness, the in-orifice shear-layer dynamics, and the acoustic-induced mass flow rate along the liner [12]. Experimental access to this near-wall region remains limited, although previous micro-PIV and LDV measurements have provided important insight into the near-orifice dynamics and acoustic-induced aerodynamic response of liners under grazing flow [13], [14]. In particular, the effect of acoustic source location on the phase-resolved velocity field in the immediate vicinity of individual perforations remains poorly documented experimentally.

The present study addresses this gap through a high-resolution LDV investigation of the near-orifice velocity field over an acoustic liner subjected to grazing turbulent flow. The measurements are used to reconstruct the acoustic-induced velocity field in the immediate vicinity of the liner perforations for different acoustic-source positions. Particular attention is paid to the extraction of acoustic quantities from LDV signals, including amplitude and phase information, in order to separate the deterministic acoustic response from the turbulent background fluctuations. To the authors' knowledge, this provides one of the first phase-resolved experimental descriptions of the micro-scale velocity field near liner perforations under grazing flow with varying source position. The objective is to clarify the local flow-acoustic mechanisms controlling liner response and to provide experimental data for the improvement of impedance eduction methods and reduced-order models.

2. Experimental setup

The tested sample corresponds to a reference geometry that has been extensively investigated across multiple experimental facilities and numerical studies [8], [12], [15]. It consists of an array of 12 cavities in the streamwise direction for a total length of L = 150 mm, and 4 in the spanwise direction for a total length of 50 mm. Each cavity is square, with a lateral dimension of $\approx 10mm$ and a depth of 38.1 mm, and contains 8 uniformly distributed orifices, as shown in Fig. 1.
The perforated plate has a thickness of 0.635 mm, while each orifice has a diameter $d \approx 1mm$, resulting in an overall porosity of 3.95%. The associated resonance frequency of the system is approximately $f_0 = 1450$ Hz.

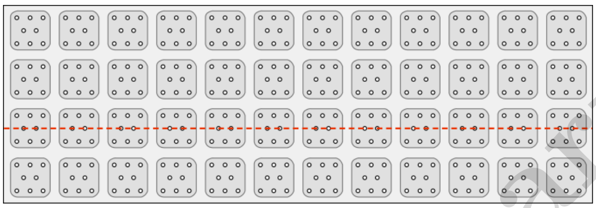

Figure 1: Liner top view with internal cavity contour and in red the LDV measurement line at 1 mm from the surface.

Experiments are conducted in the Aero-Thermo-Acoustic facility B2A at ONERA, shown in Fig. 2, which is designed to investigate liner-flow-acoustic interactions under controlled grazing-flow conditions [7]. The test section consists of a square duct of 50 mm cross section in which a fully developed turbulent boundary layer is established over an acoustic liner mounted flush with the lower wall. This configuration is representative of canonical grazing-flow liner studies, where the coupling between the boundary layer and the lined wall governs the acoustic response [3], [10], [12]. Flow conditions are controlled and monitored to ensure repeatability at a temperature of $20°C$ and a Mach = 0.3 resulting in a central streamwise mean velocity $U_0 = 110m.s^{-1}$.
The acoustic excitation is provided by loudspeakers connected to the duct at 1.3 m from the lined section, either upstream or downstream. This configuration allows investigation of the influence of source direction with respect to the mean flow on the local flow-acoustic

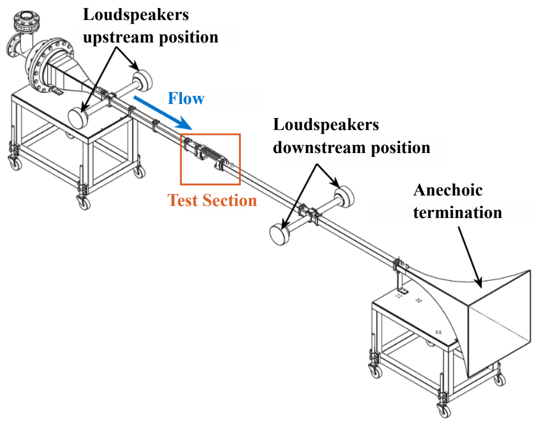

Figure 2: Schematic of the B2A duct.

coupling and on the resulting acoustic response. The acoustic signal is a single tone at 1500 Hz and is used as a reference for phase-resolved measurements, following standard approaches in duct acoustics and impedance eduction [16]. The acoustic signal is set to an incident SPL of 145 dB, resulting in a total SPL of approximately 149 dB, as observed in Fig. 4.
The main operating conditions for this study are summarized in Table 1.

Table 1: Summary of the LDV experimental test matrix.

	Case 1	Case 2
Mach	0.3	0.3
Acoustic source	Upstream	Downstream
Tonal frequency	1500 Hz	1500 Hz
Incident SPL	145 dB	145 dB

Velocity measurements are performed using laser doppler velocimetry, providing non-intrusive, high-resolution access to the streamwise and wall-normal velocity components in the vicinity of the liner surface [14]. Particular attention is given to the near-orifice region, where measurement points are distributed with fine spatial resolution to capture the local flow development above the perforations, following the physical insight provided by near-orifice measurements of liner response [13]. The LDV signals are processed with an in-house Python script to obtain the mean velocity and the root-mean-square (RMS) of the fluctuating velocity.
In addition, the acoustic velocity signal is extracted from the LDV measurements using a cross-correlation with the reference excitation signal following the work of Leon et al [17]. This method allow the determination of both the amplitude and phase of the acoustic velocity fluctuations in addition to confidence intervals. This methodology provides a phase-resolved characterization of the flow–acoustic interaction at the orifice scale.
The LDV measurement volume was approximately 70 μm in the streamwise and wall-normal directions, with a spanwise averaging length of approximately 700 μm. Measurements were performed as close as

possible to the liner surface, with the lowest reliable measurement height around 0.6 mm above the surface depending on optical access and seeding quality.
The LDV measurements were performed in two steps. First, Measurements were performed along the whole liner on a line represented on Fig. 1 at $y/d \approx 1$ over the liner to characterize the flow and acoustic response in the near vicinity of the liner. Then, Measurements were performed on a refined mesh above a single orifice represented on Fig. 3. The location of the orifice to be studied is chosen using the results from section 3.1. The refined measurements above the selected orifice were performed over a two-dimensional grid extending from approximately $y/d \approx 0.5-1$ above the liner surface and from approximately $x/L \approx 0.597-0.617$.

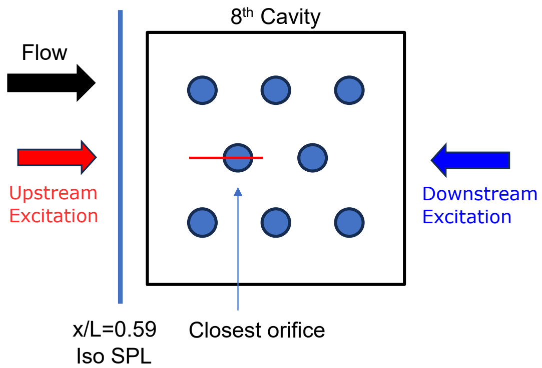

Figure 3: Schematic of the near orifice location with in red the LDV measurement line above.

3. Results and discussion

This section first presents the wall-pressure and velocity fields measured along the liner for upstream and downstream source positions, before focusing on a refined mesh near a selected orifice.

3.1. Wall-pressure measurements along the sample

The total SPL measured at the wall opposite to the liner is shown in Fig. 4 for a pure-tone excitation at 1500 Hz, close to the liner resonance frequency.
The streamwise SPL evolution differs between the two source positions. In particular, the attenuation along the liner is stronger for the downstream-source configuration than for the upstream-source configuration. This asymmetric decay in the presence of grazing flow is consistent with the behavior reported by Paduano et al [12]. A specific location of interest is found where the two total-SPL curves intersect. This location is found at $x/L \approx 0.6$ is located between the 7th and 8th cavities shown in Fig. 1. The orifice closest to this position is therefore selected for the refined LDV measurements discussed in the following sections and represented on Fig. 3.

3.2. Flow statistics along the liner

Measurements distributed in the streamwise direction at a given height of 1 mm are first examined to compare the flow statistics obtained for the two acoustic source positions.

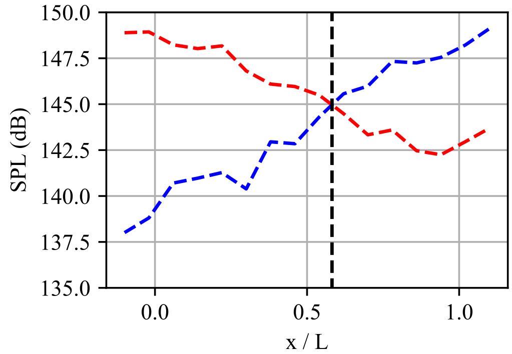

Figure 4: SPL decay along the liner sample for the upstream (in red) and downstream (in blue) source positions.

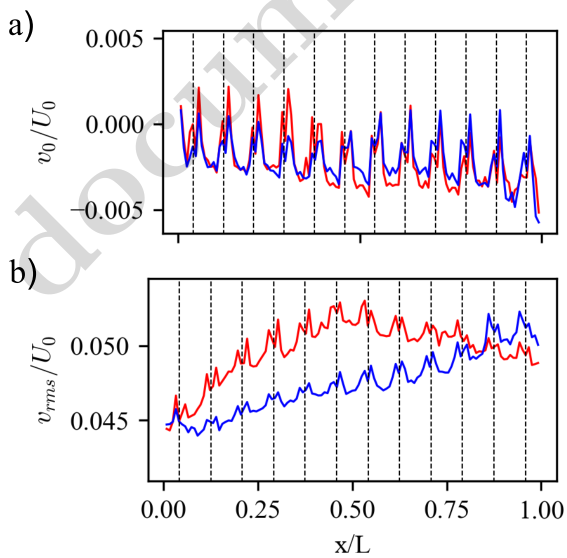

Figure 5: a) Mean wall-normal velocity and b) RMS of the wall-normal fluctuations, both normalized by U_0, along the liner at 1 mm from the surface for the upstream (in red) and downstream (in blue) source positions.

The streamwise distribution of the mean wall-normal velocity v_0 is shown in Fig. 5a. Values remain close to zero over the rigid section, typically below 1% of the mean streamwise velocity, representative of channel flows. Over the liner, local variations coincide with orifice locations, suggesting an acoustically induced wall-normal bias flow.
The wall-normal velocity fluctuations, quantified by $v'_{\mathrm{rms}}(x)$ and shown in Fig. 5b, reflect the development of the grazing turbulent boundary layer in the presence of acoustic excitation [14]. Local peaks align with the orifice positions, with increased fluctuations over the lined section due to acoustic forcing, followed by a gradual attenuation consistent with liner damping.
A directional dependence of the flow response is al-

ready observed in these measurements, especially near the streamwise location where similar SPL values are measured at the opposite wall, around $x/L \approx 0.6$. The closest orifice to this position is therefore selected for the remainder of the study to investigate the effect of acoustic source position.

3.3. Influence of the acoustic source position on flow statistics above an orifice

The rest of the study focuses on a single orifice. The orifice was chosen as the closest orifice to the $x/L \approx 0.6$ location as represented on fig 3.

A first indication of source-location dependency is obtained from the fluctuation levels measured on a refined mesh near the selected aperture. Measurements are performed $y/d \approx 0.5$ above the liner surface and are examined along a streamwise line over the orifice. The RMS velocity fluctuations are shown in Fig. 6. The streamwise component exhibits distinct behavior for the two source positions, indicating different states of the tangential flow developing over the liner, as also observed in recent LDV measurements addressing source-location effects [14]. This difference may be associated with the modification of the near-wall shear strength at this location [12].

The wall-normal component shows a similar source-position dependence, with a peak over the orifice that reflects oscillatory motion through the aperture and momentum injection into the grazing flow, consistent with the near-orifice dynamics reported by [13].

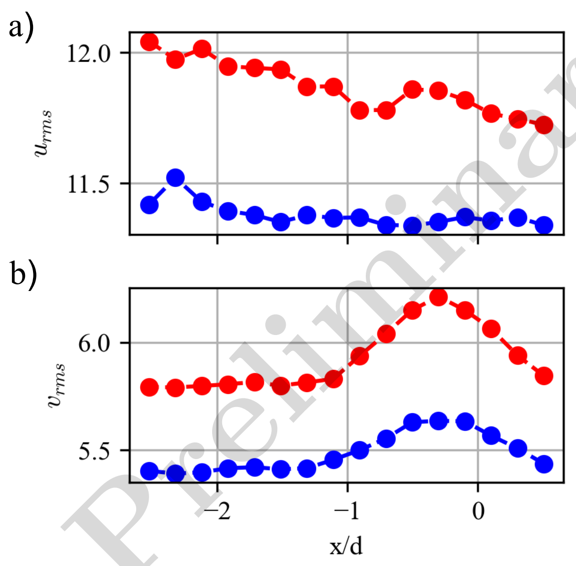

Figure 6: a) Streamwise and b) wall-normal RMS velocity near the selected orifice for the upstream (in red) and downstream (in blue) source positions.

3.4. Influence of the acoustic source position on acoustic dynamics above an orifice

For harmonic forcing, the complex amplitudes $\hat{u} = |\hat{u}|e^{i\phi_u}$ and $\hat{v} = |\hat{v}|e^{i\phi_v}$ define the polarization (shape and orientation) of the periodic trajectory followed by the coherent velocity vector in the (u,v) plane. This polarization depends on both the relative amplitudes of the two components and their phase difference.

Figure 7 presents the amplitude of the coherent velocity components above the selected orifice. The streamwise component exhibits a local decrease in the vicinity of the aperture, followed by a recovery downstream of the orifice. This behavior suggests a local modification of the coherent velocity field as the acoustic motion interacts with the aperture and the grazing boundary layer. In contrast, the wall-normal component shows a localized increase over the aperture, consistent with an enhanced oscillatory motion normal to the liner surface.

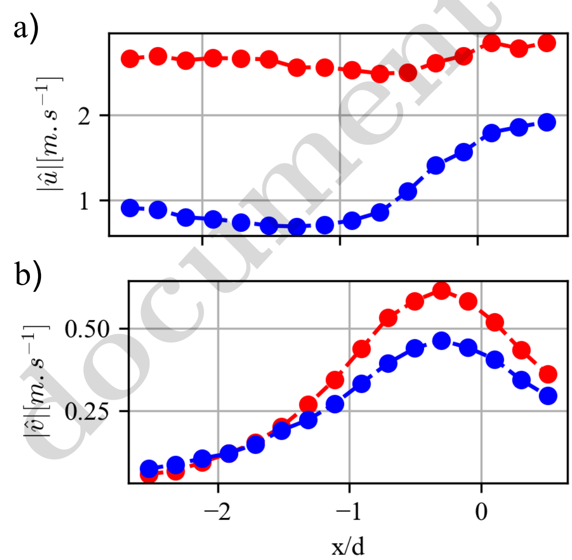

Figure 7: a) Streamwise and b) wall normal coherent reconstructed velocity amplitude near the selected orifice for the upstream (in red) and downstream (in blue) source positions.

A clear dependence on the acoustic source position is observed. At this streamwise location, the streamwise coherent velocity amplitude is larger for the upstream-source configuration than for the downstream-source configuration, in agreement with the expected sensitivity of the near-wall acoustic velocity field to the direction of acoustic propagation under grazing-flow conditions [12], [18]. Away from the aperture, the wall-normal component remains of comparable magnitude for the two source positions. However, the local maximum observed over the aperture is more pronounced for upstream forcing, suggesting a stronger local wall-normal coherent motion in this configuration.

The local phase difference, $\Delta\phi = \phi_u - \phi_v$, is used to complement the amplitude analysis. Values close to $0°$ or $180°$ correspond to an approximately rectilinear trajectory, whereas values approaching $\pm 90°$ indicate a more elliptical trajectory. As shown in Fig. 8, the downstream-source case remains close to zero over most of the region, while the upstream-source case approaches quadrature over part of the aperture. Together with Fig. 7, this result suggests that the acoustic source position affects not only the magnitude of the coherent velocity components, but also their relative phase of the near-orifice acoustic velocity field. This behavior is consistent with a source-direction-dependent coupling between the grazing shear flow and the acoustic motion near the aperture.

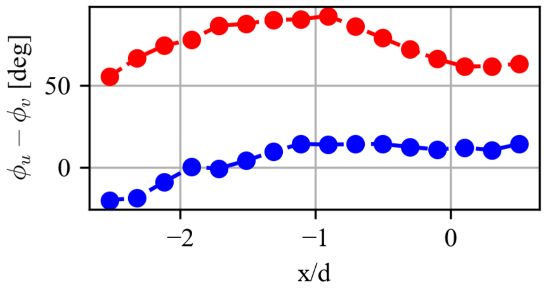

Figure 8: Phase shift between streamwise and wall-normal coherent velocity components near the selected orifice for the upstream (in red) and downstream (in blue) source positions.

3.5. Acoustic velocity indicators

From the complex coherent velocity components, several integral indicators are defined over a two-dimensional region above the streamwise projection of the selected orifice to help describe the acoustic dynamics. This region, denoted by A_o, extends on the full 2D mesh defined at the end of section 2. The use of a two-dimensional integration domain reduces the sensitivity of the indicators to local positioning uncertainties.

A first quantity is the complex wall-normal motion proxy:

$$\hat{Q}v = \iint_{A_o} \hat{v}(x, y), \mathrm{d}x, \mathrm{d}y,$$

which measures the coherent wall-normal motion induced above the aperture. Although it does not correspond to the true volumetric flux through the orifice, it provides a consistent proxy for the local pumping strength of the liner surface.

To characterize the coupling between the two velocity components, we introduce the complex correlation :

$$\hat{C}uv = \iint_{A_o} \hat{u}(x, y)\hat{v}^*(x, y), \mathrm{d}x, \mathrm{d}y.$$

This quantity captures the amplitude and phase relationship between streamwise and wall-normal motions as well as their coherent coupling.

A scalar indicator of the relative orientation of the velocity field is defined as

$$R = \frac{E_v}{E_u} = \frac{\iint_{A_o} |\hat{v}(x, y)|^2, \mathrm{d}x, \mathrm{d}y}{\iint_{A_o} |\hat{u}(x, y)|^2, \mathrm{d}x, \mathrm{d}y}.$$

This ratio quantifies whether the coherent motion above the orifice is predominantly wall-normal or streamwise. Variations of R between the two source positions indicate changes in the shape and orientation of the periodic trajectory followed by the coherent velocity vector.

These indicators are computed for the two acoustic source configurations and are presented in Table 2 as upstream-to-downstream amplitude ratios and phase differences.

Table 2: Upstream-to-downstream comparison of the acoustic velocity indicators above the selected orifice.

Upstream to downstream comparison	Value
Amplitude ratio $\lvert Q_v \rvert$ (up / down)	1.23
Amplitude ratio $\lvert C_{uv} \rvert$ (up / down)	2.76
Energy ratio R (up / down)	3.16
Phase shift Q_v [deg] (up - down)	48
Phase shift C_{uv} [deg] (up - down)	-62

The indicators in Table 2 highlight a source-position dependence of the coherent velocity field above the selected orifice. The wall-normal flux proxy is about 23% larger for upstream forcing, consistent with the amplitude distributions in Fig. 7b. The larger variation of $|\hat{C}_{uv}|$ and of the energy ratio (R) suggests that the main difference between the two cases is not only the wall-normal amplitude, but also the coupling and relative orientation of the streamwise and wall-normal coherent motions. The phase shifts of $\hat{Q}v$ and $\hat{C}uv$ are consistent with a source-direction-dependent acoustic response of the orifice under grazing flow.

4. Conclusion

This study investigated the influence of acoustic source location on the near-orifice flow and coherent velocity field over a liner under grazing turbulent flow using LDV measurements. The results indicate that both the flow statistics and the reconstructed coherent velocity field are sensitive to the direction of acoustic propagation. Local variations are observed near the orifice, including changes in wall-normal fluctuations, coherent velocity amplitudes, and phase relationships. The phase-resolved analysis suggests that the source position affects not only the magnitude of the acoustic-induced velocity components, but also the shape and orientation of their periodic trajectory above the aperture. The integral indicators further support this source-dependent response, with larger wall-normal motion and stronger streamwise/wall-normal coupling for the upstream-source case.

These findings provide experimental evidence for source-position effects in the local liner-flow-acoustic interaction. Future work will extend the database to more complex liner geometries and multiple-orifice configurations, with the aim of supporting time-domain impedance eduction approaches based on local flow-acoustic measurements.

5. Acknowledgments

The work of L. Ambrosiani is co-funded by ONERA and the European Union (ERC, LINING, 101075903). The work of F. Avallone is co-funded by the European Union (ERC, LINING, 101075903). Views and opinions expressed are, however, those of the author(s) only and do not necessarily reflect those of the European Union or the European Research Council. Neither the European Union nor the granting authority can be held responsible for them. The authors thank the AeroAcoustics Research Consortium (AARC) for sharing the liner geometry. The AARC is a government-industry partnership supporting pre-competitive research for aircraft noise reduction.

References

[1] R. E. Motsinger and R. E. Kraft, "Design and performance of duct acoustic treatment," in *Aeroacoustics of Flight Vehicles: Theory and Practice, Volume 2: Noise Control*, NASA Langley Research Center, 1991.

[2] X. Ma and Z. Su, "Development of acoustic liner in aero engine: A review," *Science China Technological Sciences*, vol. 63, no. 12, pp. 2491–2504, Dec. 2020, ISSN: 1869-1900. DOI: 10.1007/s11431-019-1501-3.

[3] Y. Auregan, R. Starobinski, and V. Pagneux, "Influence of grazing flow and dissipation effects on the acoustic boundary conditions at a lined wall," *The Journal of the Acoustical Society of America*, vol. 109, no. 1, 2001.

[4] E. J. Brambley, "Well-posed boundary condition for acoustic liners in straight ducts with flow," *AIAA Journal*, vol. 49, no. 6, pp. 1272–1282, 2011. DOI: 10.2514/1.J050723.

[5] S. W. Rienstra and M. Darau, "Boundary-layer thickness effects of the hydrodynamic instability along an impedance wall," *Journal of Fluid Mechanics*, vol. 671, pp. 559–573, 2011. DOI: 10.1017/S0022112010006051.

[6] R. Roncen, E. Piot, F. Mery, F. Simon, M. Jones, and D. Nark, "Wavenumber-based impedance eduction with a shear grazing flow," *AIAA Journal*, vol. 58, pp. 1–11, Apr. 2020. DOI: 10.2514/1.J059100.

[7] V. Lafont, F. Méry, R. Roncen, F. Simon, and E. Piot, "Liner impedance eduction under shear grazing flow at a high sound pressure level," *AIAA Journal*, vol. 58, no. 3, pp. 1107–1117, 2020. DOI: 10.2514/1.J058756.

[8] N. T. Quintino et al., "Comparison of impedance eduction test rigs with different boundary-layer profiles," *AIAA Journal*, pp. 1–12, 2025. DOI: 10.2514/1.J065173.

[9] F. Avallone, A. Khedr, A. Paduano, F. Scarano, L. Meirelles, and J. Cordioli, "On the relevance of facesheet orifice geometry to acoustic liner impedance," *npj Acoustics*, vol. 2, p. 6, 2026. DOI: 10.1038/s44384-026-00044-x.

[10] Q. Zhang and D. J. Bodony, "Numerical investigation of a honeycomb liner grazed by laminar and turbulent boundary layers," *Journal of Fluid Mechanics*, vol. 792, pp. 936–980, Mar. 2016. DOI: 10.1017/jfm.2016.79.

[11] F. Avallone and D. Casalino, "Acoustic-induced velocity in a multi-orifice acoustic liner grazed by a turbulent boundary layer," in *AIAA Aviation and Aeronautics Forum and Exposition, AIAA AVIATION Forum 2021*, American Institute of Aeronautics and Astronautics Inc. (AIAA), 2021.

[12] A. Paduano, F. Scarano, J. Cordioli, D. Casalino, and F. Avallone, "On the impact of the turbulent grazing flow development on the acoustic response of an acoustic liner," *Journal of Fluid Mechanics*, vol. 1035, A11, 2026. DOI: 10.1017/jfm.2026.11544.

[13] O. Léon, F. Mery, E. Piot, and C. Conte, "Near-wall aerodynamic response of an acoustic liner to harmonic excitation with grazing flow," *Experiments in Fluids*, vol. 60, Aug. 2019. DOI: 10.1007/s00348-019-2791-5.

[14] L. Ambrosiani, E. Piot, F. Méry, and F. Avallone, "Laser doppler velocimetry measurements of acoustic–turbulent flow interaction over a liner," in *32nd AIAA/CEAS Aeroacoustics Conference*, Brussels, Belgium, 2026. DOI: 10.2514/6.2026-3201.

[15] F. Avallone et al., "On the comparison of different methods for impedance eduction applied to a numerical database," in *30th AIAA/CEAS Aeroacoustics Conference*, 2024. DOI: 10.2514/6.2024-3294.

[16] J. Primus, E. Piot, and F. Simon, "An adjoint-based method for liner impedance eduction: Validation and numerical investigation," *Journal of Sound and Vibration*, vol. 332, no. 1, pp. 58–75, 2013, ISSN: 0022-460X. DOI: 10.1016/j.jsv.2012.07.051.

[17] O. Léon, E. Piot, D. Sebbane, and F. Simon, "Measurement of acoustic velocity components in a turbulent flow using LDV and high-repetition rate PIV," *Experiments in Fluids*, vol. 58, p. 72, May 2017. DOI: 10.1007/s00348-017-2348-4.

[18] F. Scarano, A. Paduano, and F. Avallone, "Noise dissipation mechanisms in a multi-cavity acoustic liner grazed by turbulent flow and acoustic waves," in *32nd AIAA/CEAS Aeroacoustics Conference (2026)*, 2026, p. 3200.